Energy Engineering

Tech Science Press

DOI: 10.32604/ee.2023.029167

ARTICLE

Emergency Energy Management of Microgrid in Industrial Park Based on Robust Optimization

Haoliang Yang*, Yonggang Dong and Zhifang Yang

Department of Electrical Engineering, Hebei Vocational University of Technology and Engineering, Xingtai, 054000, China

*Corresponding Author: Haoliang Yang. Email: yanghl202204@163.com

Received: 05 February 2023 Accepted: 25 May 2023 Published: 29 November 2023

ABSTRACT

Reducing the impact of power outages and maintaining the power supply duration must be considered in implementing emergency energy dispatching in micro-networks. This paper studies a new emergency energy treatment method based on the robust optimal method and the industrial park micro-network with the optical energy storage system. After controlling the load input, a control strategy of adjusting and removing is proposed. Rolling optimal theory is applied to emergency energy scheduling based on a robust optimal mathematical model. A weighting factor is introduced into the optimal model to balance the importance of reducing and retaining the power supply. Uncertainty is designed to adjust the effect of uncertainty on the problem. The example shows that this method can flexibly set the weight coefficient and uncertainty value according to the actual situation so that the input of the control load can be optimized.

KEYWORDS

Robust optimal; weighting coefficient; emergency energy sources; rolling optimization; microgrid in an industrial park

1 Introduction

New energy vehicles have developed rapidly due to their safety, convenience, high efficiency, and environmental protection. Although there are essential differences between modern and traditional vehicles in power, the fundamental nature of new vehicles is still derived from the upgrading and transformation of conventional cars. The high-speed rotation of the motor and air-conditioning condensers are still the two significant cooling needs of new energy vehicles. In addition, the cooling part of the battery is also increased, so the new energy vehicle contains four discrete, independent cooling systems: power supply, motor, electric control, and air conditioning. The four parts are separate and do not interfere with each other. This content brings many consumables, occupies space, causes energy consumption, and causes other problems. Limited by the current technology, the battery life, driving capacity, and vehicle performance of new energy vehicles must be improved by various means. Theoretically, the four cooling systems also have the optimization potential of saving material, energy, and space. Vehicle coordination, system integration, and humanized experience will be the future development direction of new energy vehicles.

Distributed generation (DG) is a way to maximize the use of renewable energy sources. DG is a primary significant measure to save energy and reduce energy consumption in the country, as well as an efficient combined energy system. Due to external conditions, photovoltaic (PV), wind power and

so on have specific intermittent and random characteristics. DG varies greatly, and its oscillation is irregular. DG brings difficulties to energy management and optimal dispatching of the micro energy grid. Considering the influence of uncertainty, it can be divided into two types: one is to use backup resource regulation to smooth the power output to meet the load demand, but its economic benefits are not ideal. The second is the analysis using stochastic optimization techniques and probabilistic statistics. Robust optimization theory is a relatively perfect theory for solving fuzzy optimization problems developed in random optimization and fuzzy optimization in the past 40 years. Robust optimality is the constraint condition that can be satisfied by constructing an uncertain set of definite intervals when all possible uncertain variables are given in a given set.

Reference [1] firstly established a naturally determined and systematic control of multiple decision variables as a robust optimal game for game players. Reference [2] introduced a robust optimal planning algorithm considering wind speed uncertainty. It uses the vital duality principle of linear optimization to transform the optimal robustness problem into hybrid linear programming. Reference [3] proposed a robust voltage control method for power systems, considering the power systems' uncertainty of capacity and loads. This method can keep PV and load stability in the case of varying concentrations. Reference [4] introduced a robust energy control method. The scenario is generated by interval fuzzy modeling, which changes the initial robust optimal problem into quadratic conic programming. Reference [5] used a two-stage robust optimal strategy to solve the uncertainty problem for grid-connected microgrids containing generators, renewable energy and energy storage systems (ESS). ESS will reduce the average operating cost. Some unit combination and economic scheduling results have been obtained with robust optimal methods. However, the current research results rarely apply the robust algorithm to the emergency energy treatment of micro-networks. Under conventional conditions, a commercial building microgrid (CBMG) is a new and sustainable power system in the industrial park. ESS island is used for emergency treatment in case of a power grid accident. However, there are still some uncertain factors in PV power generation capacity after CBMG transitions to the island. Reasonable control of unstable energy is of great significance to ensure the safe and stable operation of the power grid.

This paper presents a robust optimal strategy for emergency energy dispatching (RO-EEM) after a power outage. This method can reduce the disturbance of power interruption to users and extend the power supply duration. A weight factor is introduced in RO-EEM to balance the importance of the two subitems. In this paper, uncertainty is introduced to improve the effect of uncertainty on the problem [6]. The control strategy of "adjusting first and then cutting off" is proposed to control the input of each period of the control load. Electric vehicles (EVs) use a two-stage adjustment during the adjustment period. Air conditioning uses cycle adjustment.

2 CBMG Architecture

CBMG consists of PV, ESS, EV, Alternating Current (AC)/DC, load, microgrid central controller (MGCC), etc. The lower machine controller consists of a micro-source controller, a load controller (LC) and an EV controller (Fig. 1).

MGCC mainly monitors and coordinates the running status of each system. It can integrate everything. The lower-level controller periodically sends data such as power consumption and generation to the MGCC. MGCC will filter and process this to control CBMG effectively. AC/DC, a bidirectional conversion circuit, can complete the DC and AC two kinds of power conversion [7]. Loads are divided into control and focus categories according to their importance and ability to be adjusted. Control loads include air conditioning, EV, auxiliary lighting, etc. It has low importance and good adjustability.

The micro-energy grid must obey the unified control of MGCC during operation, but the size of its adjustment significantly impacts the system use effect. The main load has the necessary lighting equipment, computer control module, etc. Its importance is higher, and its adjustability is lower. In operating a micro energy grid, the stable power supply should be kept as far as possible. If MGCC still cannot meet the requirements of the main load after adjustment, it will significantly affect the safe and stable operation of the whole power grid [8].

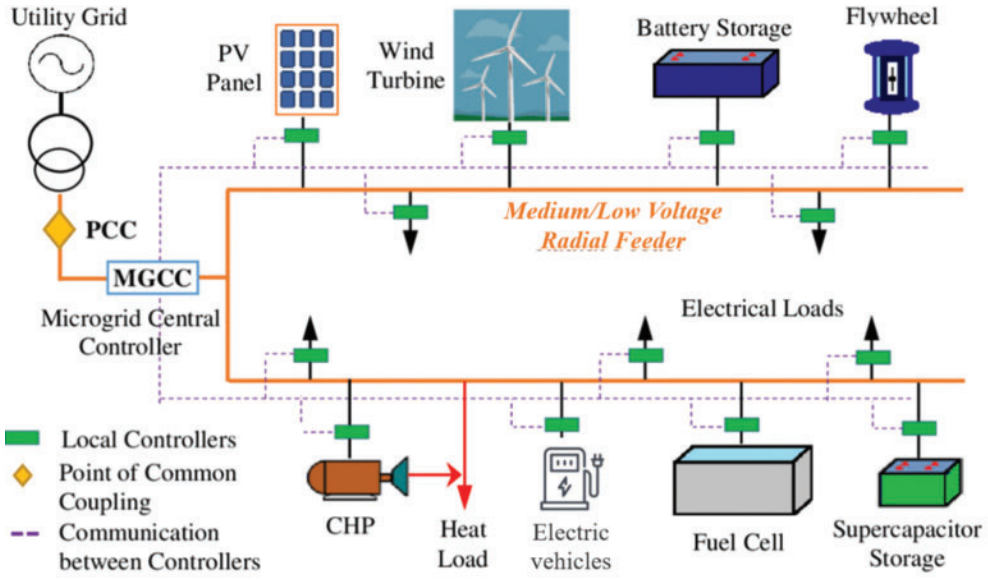

Figure 1: Schematic diagram of a micro-network system in optical energy storage Industrial Park

3 Mathematical Modeling

The CBMG will go to an island state after a power outage in the distribution network. Given the V/F control situation, no matter how the input and output power of the battery energy storage system changes, the voltage and frequency output by the inverter are given values. The difference between the measured frequency f and the reference frequency determines frequency control. Then the phase angle of the inverter is controlled by the proportional-integral regulator output. The output voltage and frequency are controlled at a given value according to the amplitude and frequency of the measured grid voltage. This keeps the grid voltage and frequency stable. Therefore, the CBMG is the primary control device in the V/F mode in the island state.

3.1 Optimization Mode

CBMG needs to consider customer satisfaction and time of use in emergencies. And the two are in conflict. The weighting factor is incorporated into the optimal index to measure its importance. Its purpose function is as follows:

$$\min ah(x) + b\tau(x) \tag{1}$$

$$h(x) = \sum_{i=1}^{n} \frac{x_{\varepsilon 0} - x_{\varepsilon i}}{x_{\varepsilon 0}} \tag{2}$$

$$\tau(x) = \sum_{i=1}^{n} \frac{SOC_0 - SOC_i}{SOC_0} \tag{3}$$

$$SOC_i = SOC_0 - \sum_{j=1}^{i} \frac{pr_j \cdot \Delta t}{A_n} \tag{4}$$

$h(x)$ represents the relative change in the controllable load. The trimmer $h(x)$ is, the closer the controllable load input is to the initial value during a power outage [9]. At this time, the less impact the power failure brings to the user, the higher the user satisfaction. The weight factor a indicates its importance. $\tau(x)$ represents the relative change in the system on a Chip (SOC) of ESS. The smaller $\tau(x)$ is. The larger the SOC of the ESS. The more backup power it can provide. Its importance is indicated by the weight factor b. The sum of the weighting factors a and b is 1. If the ESS stores more standby energy, the user has less dependence on controllable load. The weight factor a should be a small value, otherwise b should be a small value. i is the number of optimizations. n is the total number of optimizations. $x_{\varepsilon 0}$ is the input of controllable load when power failure occurs. $x_{\varepsilon i}$ is the input of controllable load in optimization i. SOC_0 is the SOC of the ESS when the outage occurs. SOC_i is the SOC of ESS at optimization i. pr_j is the discharge power of ESS at the JTH optimization. Δt is the time interval between two adjacent optimizations. A_n is the rated capacity of ESS.

3.1.1 Constraints on Power Balance

The discharge power of ESS must meet Eq. (5). The purpose is to maintain the power balance of the System after CBMG switches to island operation.

$$pv_i + pr_i = x_{\varepsilon i} + x_{\varepsilon ri} \tag{5}$$

pv_i is the predicted value of PV in optimization i. $x_{\varepsilon ri}$ is the necessary load at the i optimization. The amount of access to critical loads is a known constant that fluctuates with time.

3.1.2 Constraints on Controllable Load

The controllable load should be adjusted within a specific range. It can be expressed as

$$x_{\varepsilon\,\min} \le x_{\varepsilon i} \le x_{\varepsilon\,\max} \tag{6}$$

$$x_{\varepsilon\,\min} = L_{\varepsilon v\min} + L_{\varepsilon t\min} + L_{\varepsilon r\min} \tag{7}$$

$$x_{\varepsilon\,\max} = L_{\varepsilon v\max} + L_{\varepsilon t\max} + L_{\varepsilon r\max} \tag{8}$$

$x_{\varepsilon\,\min}$ and $x_{\varepsilon\,\max}$ are the lower and upper limits of Bx_{ci}. $L_{\varepsilon v\min}$, $L_{\varepsilon t\min}$ and $L_{\varepsilon r\min}$ are the lower limits of controllable load EV, air conditioning and secondary lighting facilities. $L_{\varepsilon v\max}$, $L_{\varepsilon t\max}$ and $L_{\varepsilon r\max}$ are the upper limits of controllable load EV, air conditioning and secondary lighting facilities.

3.1.3 ESS Constraints

The SOC of ESS should be strictly controlled within a specific range. The goal is to prevent damage to ESS from overcharging and over-discharging. It can be expressed as

$$SOC_{\min} \le SOC_i \le SOC_{\max} \tag{9}$$

$SOC_{\min}$, $SOC_{\max}$ is the lower limit and upper limit of SOC_i. The discharge power of ESS also has a range limit. It can be expressed as

$$pr_{min} \le pr_i \le pr_{\max} \tag{10}$$

pr_i Positive ESS discharge. ESS is charged when it is negative. $pr_{\min}$ is the upper limit of charging power of ESS. $pr_{\max}$ is the upper limit of ESS discharge power.

PV predictions are often based on data collected over a short period. It has certain randomness and volatility [10]. The above optimization model is written in matrix form. Matrix C, matrix W_ε in the objective function, matrix K, matrix T and matrix τ in the constraint condition are free of uncertainties. Matrix k contains uncertainties. $x$is the column vector composed of controllable load input and ESS discharge power. The original optimization model can be expressed as

$$\min Wx + W_\varepsilon \tag{11}$$

s.t.

$$Kx = k \tag{12}$$

$$Tx \le \tau \tag{13}$$

$$x_{\min} \le x \le x_{\max} \tag{14}$$

Eqs. (12) and (13) in the constraint condition can be combined

$$Ax \le b \tag{15}$$

The constant term in the objective function does not affect the optimal solution. Therefore, the above optimization model can be simplified as follows:

$$\min Cx \tag{16}$$

$$Ax \le b \tag{17}$$

$$x_{\min} \le x \le x_{\max} \tag{18}$$

3.2 RO-EEM Model

When the distribution network is out, CBMG switches to island operation. If the initial SOC of ESS is small and the load is large, the PV output is higher [11]. This is more conducive to the access of controllable load and the maintenance of ESS reserve power. The worst case is the lowest PV output. PV output at a time A_i is ω_i. The fluctuation range of PV_i is $\overline{\omega}_i - \hat{\omega}_i \le \omega_i \le \overline{\omega}_i + \hat{\omega}_i$. The PV output value in the optimization model should be $\omega_i = \overline{\omega}_i - \Psi_i\hat{\omega}_i$. Ψ_i is the uncertainty at the ith moment. Ψ_i should satisfy $0 \le \Psi_i \le 1$ and $\sum \Psi_i = \Psi$. Ψ is the total uncertainty. RO-EEM model based on optimization model {(11)–(14)} can be expressed as

$$\min Cx + W_\varepsilon \tag{19}$$

s.t.

$$Kx = \overline{\omega} - diag(\hat{\omega})\Psi - x_{\varepsilon r} \tag{20}$$

$$Tx \le \tau \tag{21}$$

$$x_{\min} \le x \le x_{\max} \tag{22}$$

$$0 \le \Psi_i \le 1 \tag{23}$$

$$\sum_i \Psi_i = \Psi \tag{24}$$

$diag(\hat{\omega})$ is a square matrix with $\hat{\omega}$ as the diagonal element and the remaining elements as 0.

4 RO-EEM Strategy

RO-EEM is a rolling optimization method based on RO-EEM. Rolling optimization is an effective method in real-time problems. The forecast of PV is constantly revised to make it more consistent with the current trend. Fig. 2 shows the schematic diagram of the RO-EEM strategy [12]. The process goes like this:

(1) Obtain SOC at the initial time $t = t_0 + i - 1 \cdot \Delta t'$ of rolling optimization. t_0 is the time when the power failure occurs. i is the number of scrolling optimizations. $\Delta t'$ is the time interval between two adjacent scrolling optimizations. As the initial SOC value of this rolling optimization.

(2) Weight factor a and b, total uncertainty Ψ. The RO-EEM model calculated the controllable load input and ESS discharge power in the remaining period. The t_b in Fig. 2 is the estimated outage time.

(3) The optimization result of the RO-EEM model is based on the PV predicted value. The decision must adjust according to the actual PV output [13]. If the difference between the actual PV output and the predicted PV value is within the allowable adjustment range of ESS, it is balanced by ESS. Otherwise, it is balanced by a controllable load. If the controllable load is not balanced when wholly removed, cutting off part of the critical load is necessary.

(4) Update the real-time data and predicted value of PV and carry out the following rolling optimization.

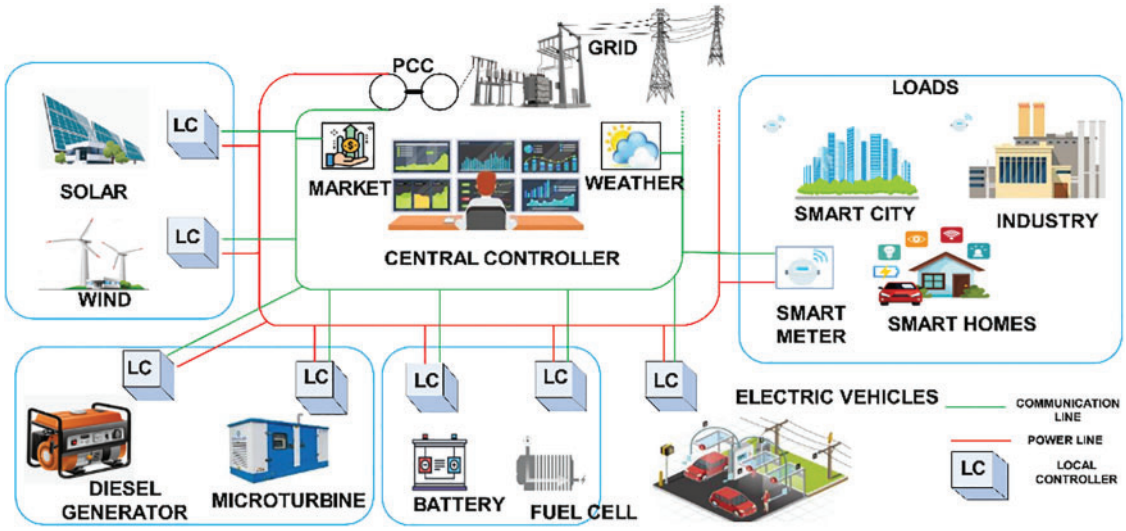

Figure 2: Schematic diagram of the RO-EEM policy

5 Specific Adjustment of Controllable Load

5.1 EV Adjustment Scheme

The relationship between SOC and charging current in the EV charging process can be expressed as Eq. (25).

$$SOC_{(EV)i+1} = SOC_{(EV)i} + \frac{I_i}{F_n}\Delta t \tag{25}$$

$SOC_{(EV)i+1}$ and $SOC_{(EV)i}$ are SOC values of EV at time $i+1$ and time i, respectively. I_i is the charging current of EV at moment i. F_n is the rated capacity of electric vehicles [14]. The charging ratio C_i of electric vehicle can be expressed as Eq. (26). Thus, SOC in the charging process of electric vehicles can be expressed as Eq. (27).

$$C_i = \frac{I_i}{F_n} \tag{26}$$

$$SOC_{(EV)i+1} = SOC_{(EV)i} + C_i \cdot \Delta t \tag{27}$$

The EV types and adjustment processes during MGCC are shown in Fig. 3. When CBMG Island operation requires EV adjustment. The flexible adjustment should be made first. Reduce its charging magnification to a minimum one by one. When the elastic adjustment period is complete, stiffness adjustment will occur if the system cannot meet the requirements. If the entire EV is cut off, the forced reduction should be used instead of truncation [15]. When EV's SOC and charge-discharge ratio are known, the flexibility-adjusted phase and stiffness-adjusted phase amplitude can be calculated by Eqs. (28) and (29).

$$P_{ri} = \sum_{r\in\Omega_r} (C_{r-i} - C_{\min}) F_n V_n \tag{28}$$

$$P_{\tau i} = \sum_{\tau\in\Omega_\tau} C_{\tau-i} \cdot F_n \cdot V_n \tag{29}$$

P_{ri} and $P_{\tau i}$ are the power adjustable ranges of the flexible and rigid adjustment stages at the ith moment respectively. Ω_r and Ω_τ are the sets of EVs that can participate in flexible and rigid regulation respectively. C_{r-i} and $C_{\tau-i}$ are the charging ratio of EV participating in flexible regulation and rigid regulation at the i moment, respectively. $C_{\min}$ is the minimum charging ratio set in advance.

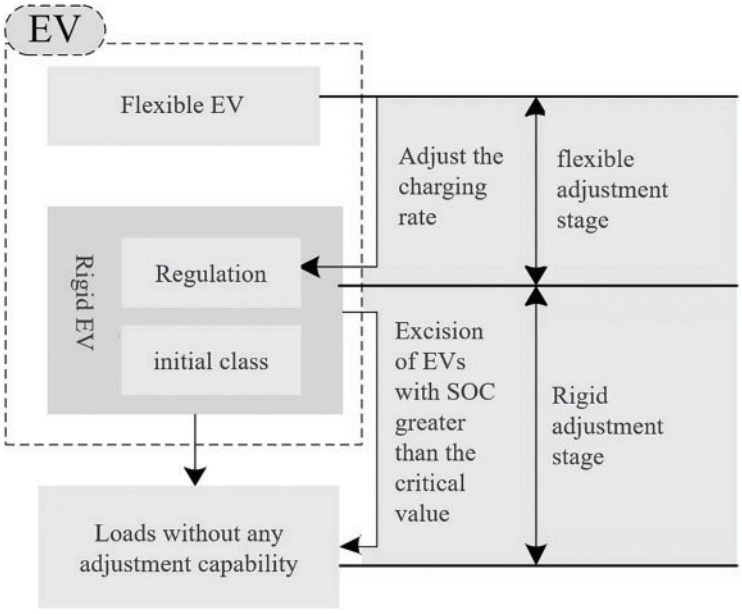

Figure 3: Types and adjustment process of electric vehicles

5.2 Air Conditioner Adjustment Scheme

The key to simulating the energy consumption of air conditioning is accurately simulating the heat exchange process. The equivalent thermal parameter model of air conditioning is shown in Fig. 4.

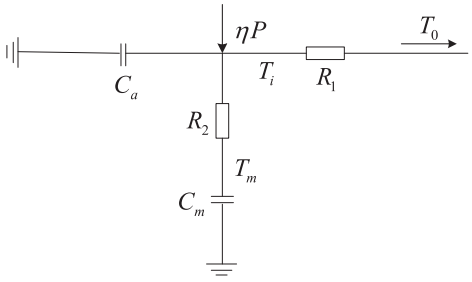

Figure 4: Equivalent thermal parameter model of air conditioning

The equivalent thermal parameter model is in Fig. 4. P is the cooling/heating power of the air-conditioning unit. η is the energy efficiency ratio. ηP is the cooling/heat production of air conditioning. C_a is the specific heat capacity of a gas. C_m is the specific heat capacity of a solid. T_o is the outside temperature. T_i is the indoor temperature. T_m is the stable indoor temperature. By simplifying the above model, we can get the calculation formula of indoor temperature T_i in steady and off states. They are shown in Eqs. (30) and (31), respectively:

$$T_i^{j+1} = T_o^{j+1} - \eta PR - \left(T_o^{j+1} - \eta PR - T_i^j\right) e^{\frac{-\Delta t}{RC}} \tag{30}$$

$$T_i^{j+1} = T_o^{j+1} - \left(T_o^{j+1} - T_i^j\right) e^{\frac{-\Delta t}{RC}} \tag{31}$$

T_i^{j+1} and T_o^{j+1} are indoor and outdoor temperatures at time j+1, respectively. C is equivalent hot melt. R is equivalent to thermal resistance. Δt is the time interval between adjacent computations.

The load response constraints under the kth anticipated accident are

$$\Delta d_{ac,t}^k \le R_{d,ac}^t \tag{32}$$

In the formula, the superscript k is the expected accident number. The power balance constraint under the kth anticipated accident is

$$-M_B^k \theta_t^k + M_H^k p_t^k = d_t - \Delta d_{ac,t}^k \tag{33}$$

The line power equation constraint under the kth anticipated accident is

$$p_{f,t}^k = M_T^k \theta_t^k \tag{34}$$

Under the kth expected accident, the upper and lower limits of line power are constrained as

$$-p_{f,\max} \le p_{f,t}^k \le p_{f,\max} \tag{35}$$

Under the kth predicted accident, the upper and lower limits of power generation are constrained as

$$q_t^k p_{\min} \le p_t^k \le q_t^k \left(p_t + R_g^t\right) \tag{36}$$

q_t^k is the start-stop state of the unit during the period t under the kth predicted accident. The problem to be solved becomes a mixed integer linear program. A mature solver can solve the system.

5.3 Controllable Load Adjustment Scheme

Through the implementation of RO-EEM, the reduction of the controllable load after each outage can be calculated compared to the initial time. The MGCC will issue tailoring orders. The basic idea of load control is to adjust before cutting [16]. As a load with a specific adjustment allowance, the CBMG air conditioning system has a better adjustment ability in the air conditioning system. Together, they will undertake the reduction of MGCCS. When the load reduction exceeds the total adjustment range of the EV and air conditioner, the load that does not have the adjustment capacity must be cut off. Non-adjustable capacity loads include secondary lighting, ultra-low SOC, and EVs with the lowest charge ratio.

6 Example Analysis

6.1 PV Prediction and Amplitude Measurement

Suppose the power goes off at 16:00. Expect a 30-min power outage. Set the interval between two adjacent scrolling optimums to 2 min. The grey algorithm makes the prediction. Many probability distributions can be approximated by using the normal distribution. Under normal conditions, the data obtained by a simple random sampling conform to the normal distribution. This property can be obtained by deducing the central limit theorem [17]. The deviation distribution of the short-term solar power forecast is close to the normal distribution because the random sampling method is adopted to sample the error of the short-term solar power forecast.

On the time axis, the mean deviation μ of the PV power generation forecast is 0. The deviation of the PV forecast is σ and the standard deviation is 0.5. The prediction error of PV follows the normal distribution of $\mu = 0$ and $\sigma = 0.5$. The maximum error δ_{max} of PV was estimated within the 95% CI range. Then the predicted change in PV is $[PV_i - \delta_{max}, PV_i + \delta_{max}]$.

6.2 Basic Data

Set the total installed capacity of PV to 100 kW. ESS is rated at 50 kWh. The maximum output of the maximum charge and discharge is 30 kW. The SOC value of ESS is 0.44 when the power is off. The highest SOC value is 0.75. The minimum is 0.11. The shortest two shortest optimal intervals A are 1 min. The main load is between 20 and 40 kilowatts, generated randomly. The maximum power of the control load is 200–500 kW. The initial setting of the control load is 200 kW.

6.3 Comparative Analysis

Comparative analysis is used in this paper. The objective is to verify the effectiveness of the RO-EEM strategy better.

6.3.1 Traditional Control Policies

CBMG systems that convert to islands after a power failure in the distribution system are complicated by their voltage/frequency changes [18]. Its charging and output can be adjusted according to load and PV changes. The control load is then progressively loaded up to the maximum output of the ESS. The input rate of the control load varies with the main load and the PV output power. At this time the result of the example is shown in Fig. 5.

As shown in Fig. 5, the ESS will not be recharged after 15 min of power failure. Photovoltaic power generation is the only power system. This will increase the risk of later stabilization operations [19]. If there is a power outage at night, the PV output will significantly reduce. It is effortless and straightforward for the ESS to stop discharging when the control load is 0 and still cannot guarantee

the need for the critical load. This will significantly adversely impact the safe and smooth operation of CBMG.

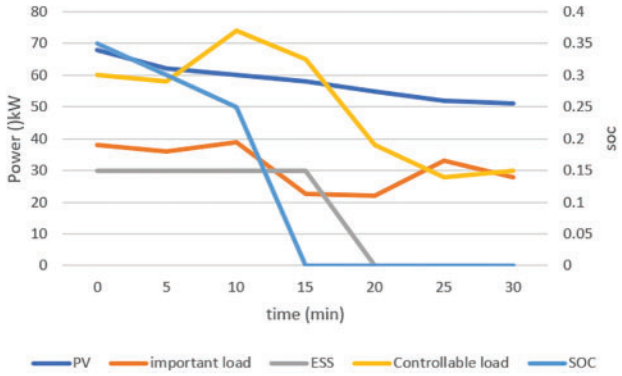

Figure 5: Schematic diagram of traditional strategy example results

6.3.2 RO-EEM Strategy

Set the weighting factor a to 0.9. b is 0.1. The population uncertainty ψ is 0. The result of the example is shown in Fig. 6. It can be seen from Fig. 6 that in the early stage of power failure, PV power is tremendous. The ESS is charging. When the power is off for 15 min, the SOC value is about 0.34. This can be prepared for future production to ensure the stable operation of CBMG. Because the blackout was at 16:00, the light was getting dimmer [20]. Therefore, the PV output power is reduced correspondingly. The discharge intensity of ESS tends to increase. Increasing the control load into the power system helps to improve customer satisfaction.

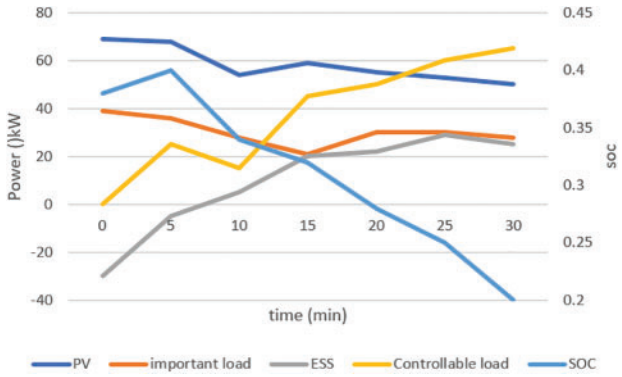

Figure 6: Schematic diagram of RO-EEM policy example results

Comparative analysis of numerical examples shows that the RO-EEM strategy can effectively adjust the input of controllable load to achieve the expected goal.

6.4 Analysis of Uncertainty Factors

In the RO-EEM model, ψ is an overall degree of uncertainty. $\psi = 0$ indicates that PV forecast at each time point is a fixed value. *a* is 0.9. b is 0.1. After obtaining various values, A's corresponding index function values are shown in Table 1. This will get worse as the uncertainty grows [21]. The decrease of PV output power to the introduction of control load and the maintenance of the backup

capacity of the ESS system will make the system users satisfied with the decrease of the ESS load. Therefore, when the value of ψ changes from 1 to 9, the value of its index function shows a trend of increasing gradually. In addition, the variation range of the PV forecast at each time point is small, so the difference in objective function value under the uncertainty condition is also low.

Table 1: Value of objective function when uncertainty ψ changes

ψ	Obj	ψ	Obj	ψ	Obj
1	22.154	4	22.169	7	22.183
2	22.159	5	22.174	8	22.188
3	22.164	6	22.178	9	22.192

6.5 Controllable Load Adjustment Results and Analysis

Set the number of electric vehicles in CBMG at 20. The default target SOC is 0.95. The SOC threshold is 0.3. Power battery parameters are shown in Table 2. EV's initial SOC is randomly generated between 0.1 and 0.6. The initial charge ratio randomly generates between 0.1 and 0.5 C (Fig. 7). The minimum EV charging ratio is set at 0.1 C in the adjustment stage.

Table 2: Power battery parameter table

Target SOC	Rated capacity	Maximum charge ratio	Rated voltage
0.95	40 Ah	0.5 C	336 V

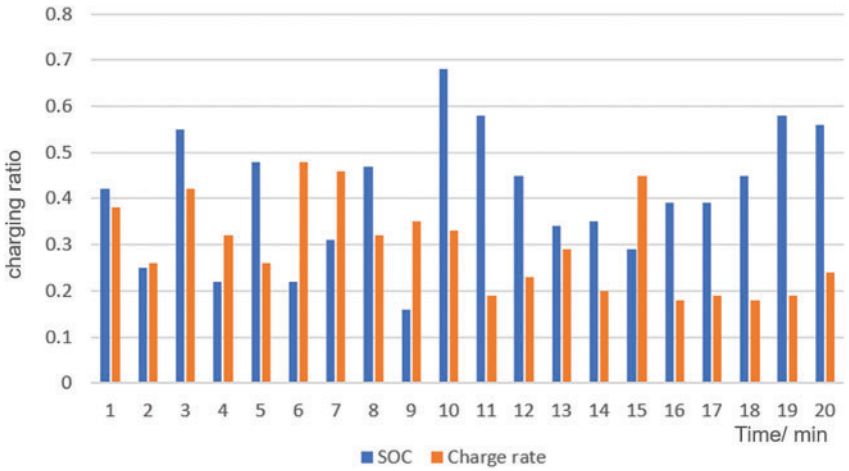

Figure 7: Initial SOC and the charging ratio of EV

Install CBMG 40 air conditioners. Its average generating capacity is 2 kilowatts. The total power at the time of the blackout was 100 kilowatts. In summer, the energy-saving effect of air conditioners reaches 3. The equivalent heat capacity is 0.18 kW/°C. When the temperature is 5.56°C/kW, the outdoor temperature does not change at 32°C. Both indoor and outdoor temperatures increase as the temperature rises [22]. The start-up setting temperature of 40 air conditioners can be arbitrarily

generated at 22°C to 28°C (Fig. 8). After the power is turned off, the indoor temperature is set the same as that of the air conditioner.

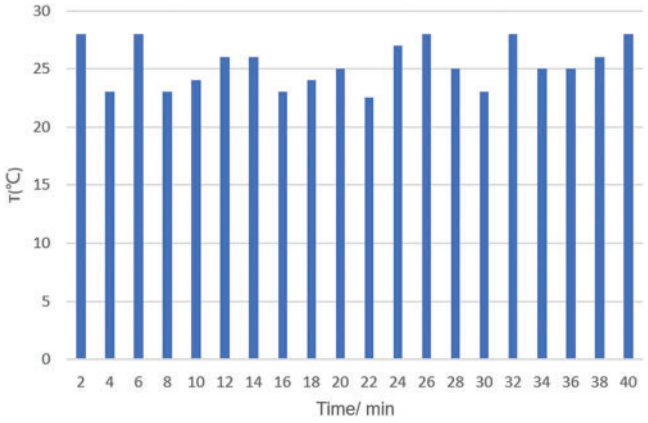

Figure 8: Randomly generated initial air conditioner temperature

When a is 0.9, b is 0.1 and ψ is 0. The RO-EEM strategy can calculate the controllable load reduction amount. Execute the reduction task according to the controllable load adjustment plan [23]. The input of EV, air conditioning and secondary lighting facilities at each moment after a power failure is shown in Fig. 9. In the early stage of power failure, the total input of controllable load is less. The air conditioning load with adjustable capacity and part of the EV are removed. Then the controllable load input showed an increasing trend. The input of air conditioning and EV increases accordingly.

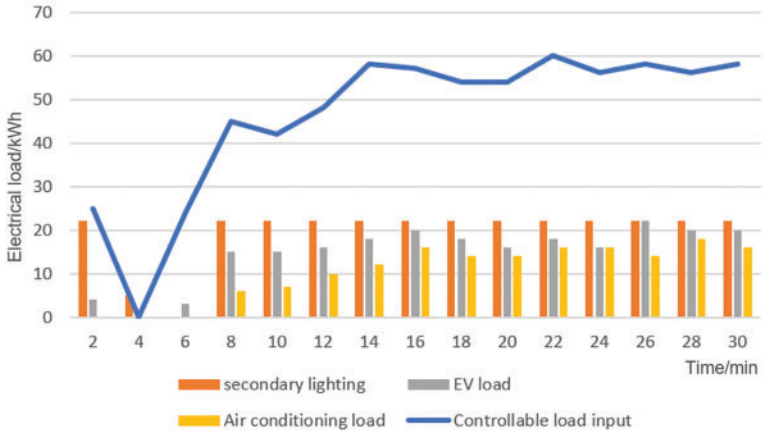

Figure 9: Input results of various controllable loads

At the initial stage of a power outage, the total input of controllable loads is small, and the air-conditioning loads and some EVs with adjustment capabilities are cut off. After that, the loadable input showed an increasing trend. The investment in air conditioners and EVs will increase accordingly. At the initial moment of power failure, the power consumption of the air conditioner is large, but because the EV contains some loads that cannot regulate. Its status is similar to that of secondary lighting facilities. It operates last when the load is reduced, so the total input amount of the EV is more than that of the air conditioner. The secondary lighting facilities have the most input due to

the lack of adjustment ability and the last action. The air conditioner is adjusted by rotation. At the initial moment of a power outage, set the odd group as the adjustable group and the even group as the removable group, and rotate every 5 min. It can be seen from Fig. 9 that the input amount of the air conditioner is 0 before the 7th min. Therefore, the temperatures of the air conditioners in the odd group and the air conditioners in the even group have risen to some extent. From the 7th min, the input of the air conditioner shows an upward trend. At this time, the odd group can be removed, and the even group can be adjusted. Therefore, between the 7th and 10th min, the temperature of the odd group of air conditioners still maintains an upward trend. In contrast, the temperature of the even group of air conditioners decreases. In the 10th, 15th, 20th and 25th min, there will be a rotation of the working mode of the odd-even group.

However, EVs adopt a two-stage adjustment when performing load reduction tasks, first reducing the charging rate and then cutting off EVs whose SOC is greater than the critical value. The EV's charging rate and SOC changes are shown in Fig. 10 during the power failure process.

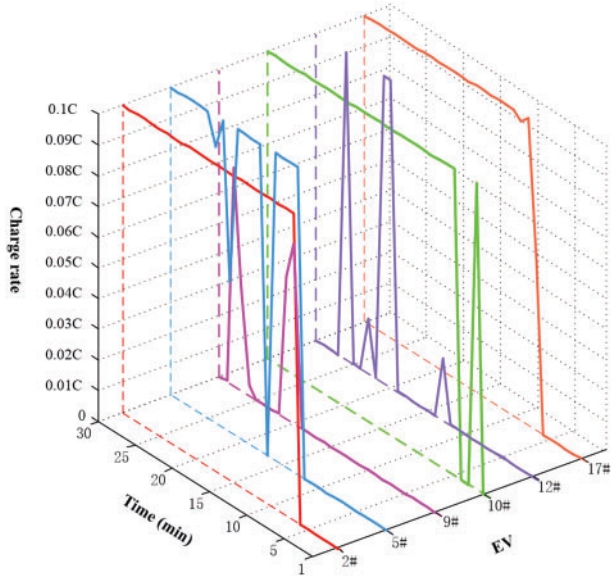

Figure 10: The EV's charging rate and SOC changes

7 Conclusion

In this paper, a robust optimization-based emergency energy management strategy is proposed. This paper adds the uncertainty factor (PV) to the optimization model. This can make the optimization result more conducive to the safe and reliable operation of the CBMG. The RO-EEM strategy introduces the idea of rolling optimization to make the predicted value of PV more in line with the actual trend. The RO-EEM strategy can effectively adjust the controllable load input. Setting different weight factors can flexibly change the importance of user satisfaction and power supply time. Each EV's real-time charging rate and air conditioning control strategy can be obtained from the controllable load adjustment scheme.

Acknowledgement: None.

Funding Statement: The authors received no specific funding for this study.

Author Contributions: The authors acknowledge the contributions to this article as follows: Study conception and design: Haoliang Yang; Data collection: Yonggang Dong; Results analysis and interpretation: Zhifang Yang; Manuscript preparation: Haoliang Yang. All authors reviewed the results and approved the final version of the manuscript.

Availability of Data and Materials: The data that support the findings of this study are available on request from the corresponding author. The data are not publicly available due to privacy or ethical restrictions.

Conflicts of Interest: The authors declare that they have no conflicts of interest to report regarding the present study.

References

1. Zhou, W., Li, Q., Wu, K., Zhang, L., Hassan, M. A. S. et al. (2022). Accelerated hierarchical optimization method for emergency energy management of microgrids with energy storage systems. *Energy Science & Engineering, 10(3),* 962–972.
2. Hashemifar, S. M. A., Joorabian, M., Javadi, M. S. (2022). Two-layer robust optimization framework for resilience enhancement of microgrids considering hydrogen and electrical energy storage systems. *International Journal of Hydrogen Energy, 47(79),* 33597–33618.
3. Wang, L., Jiang, C., Gong, K., Si, R., Shao, H. et al. (2020). Data-driven distributionally robust economic dispatch for distribution network with multiple microgrids. *IET Generation, Transmission & Distribution, 14(24),* 5712–5719.
4. Zhu, N., Hu, P., Liu, S., Jiang, D., Liang, Y. et al. (2022). Emergency reserve constrained optimal allocation of energy storage in a novel honeycomb-like microgrid cluster with volatile renewable energy resources. *IET Generation, Transmission & Distribution, 16(2),* 305–318.
5. Mallikarjunaswamy, S., Sharmila, N., Maheshkumar, D., Komala, M., Mahendra, H. N. (2020). Implementation of an effective hybrid model for islanded microgrid energy management. *Indian Journal of Science and Technology, 13(27),* 2733–2746.
6. Zhou, B., Zou, J., Chung, C. Y., Wang, H., Liu, N. et al. (2021). Multi-microgrid energy management systems: Architecture, communication, and scheduling strategies. *Journal of Modern Power Systems and Clean Energy, 9(3),* 463–476.
7. Stasinos, E. I. E., Trakas, D. N., Hatziargyriou, N. D. (2022). Microgrids for power system resilience enhancement. *iEnergy, 1(2),* 158–169.
8. Cai, S., Xie, Y., Wu, Q., Zhang, M., Jin, X. et al. (2021). Distributionally robust microgrid formation approach for service restoration under random contingency. *IEEE Transactions on Smart Grid, 12(6),* 4926–4937.
9. Masrur, H., Gamil, M. M., Islam, M. R., Muttaqi, K. M., Lipu, M. H. et al. (2022). An optimized and outage-resilient energy management framework for multicarrier energy microgrids integrating demand response. *IEEE Transactions on Industry Applications, 58(3),* 4171–4180.
10. Chen, B., Wang, J., Lu, X., Chen, C., Zhao, S. (2020). Networked microgrids for grid resilience, robustness, and efficiency: A review. *IEEE Transactions on Smart Grid, 12(1),* 18–32.
11. Islam, M., Yang, F., Amin, M. (2021). Control and optimisation of networked microgrids: A review. *IET Renewable Power Generation, 15(6),* 1133–1148.
12. Hemmati, M., Mohammadi-Ivatloo, B., Abapour, M., Anvari-Moghaddam, A. (2020). Optimal chance-constrained scheduling of reconfigurable microgrids considering islanding operation constraints. *IEEE Systems Journal, 14(4),* 5340–5349.

13. Cai, S., Zhang, M., Xie, Y., Wu, Q., Jin, X. et al. (2022). Hybrid stochastic-robust service restoration for wind power penetrated distribution systems considering subsequent random contingencies. *IEEE Transactions on Smart Grid, 13(4),* 2859–2872.
14. Vahedipour-Dahraie, M., Rashidizadeh-Kermani, H., Anvari-Moghaddam, A. (2020). Risk-based stochastic scheduling of resilient microgrids considering demand response programs. *IEEE Systems Journal, 15(1),* 971–980.
15. Liu, G., Jiang, T., Ollis, T. B., Li, X., Li, F. et al. (2020). Resilient distribution system leveraging distributed generation and microgrids: A review. *IET Energy Systems Integration, 2(4),* 289–304.
16. Daneshvar, M., Mohammadi-Ivatloo, B., Abapour, M., Asadi, S., Khanjani, R. (2020). Distributionally robust chance-constrained transactive energy framework for coupled electrical and gas microgrids. *IEEE Transactions on Industrial Electronics, 68(1),* 347–357.
17. Qiu, H., Gu, W., Xu, Y., Yu, W., Pan, G. et al. (2020). Tri-level mixed-integer optimization for two-stage microgrid dispatch with multi-uncertainties. *IEEE Transactions on Power Systems, 35(5),* 3636–3647.
18. Yang, P., Yu, L., Wang, X., Zheng, P., Lv, X. et al. (2022). Multi-objective planning and optimization of microgrid lithium iron phosphate battery energy storage system consider power supply status and CCER transactions. *International Journal of Hydrogen Energy, 47(69),* 29925–29944.
19. Vahedipour-Dahraie, M., Rashidizadeh-Kermani, H., Anvari-Moghaddam, A., Siano, P. (2020). Flexible stochastic scheduling of microgrids with islanding operations complemented by optimal offering strategies. *CSEE Journal of Power and Energy Systems, 6(4),* 867–877.
20. Rangu, S. K., Lolla, P. R., Dhenuvakonda, K. R., Singh, A. R. (2020). Recent trends in power management strategies for optimal operation of distributed energy resources in microgrids: A comprehensive review. *International Journal of Energy Research, 44(13),* 9889–9911.
21. Madiba, T., Bansal, R. C., Mbungu, N. T., Bettayeb, M., Naidoo, R. M. et al. (2022). Under-frequency load shedding of microgrid systems: A review. *International Journal of Modelling and Simulation, 42(4),* 653–679.
22. Wang, W., He, Y., Xiong, X., Chen, H. (2021). Robust survivability-oriented scheduling of separable mobile energy storage and demand response for isolated distribution systems. *IEEE Transactions on Power Delivery, 37(5),* 3521–3535.
23. Gazijahani, F. S., Salehi, J., Shafie-Khah, M., Catalão, J. P. (2020). Spatiotemporal splitting of distribution networks into self-healing resilient microgrids using an adjustable interval optimization. *IEEE Transactions on Industrial Informatics, 17(8),* 5218–5229.